Simultaneous and Proportional Real-Time Myocontrol of up to three Degrees of Freedom of the Wrist and Hand

Markus Nowak, Ivan Vujaklija, *Member, IEEE*, Agnes Sturma, Claudio Castellini, and Dario Farina, *Fellow, IEEE*

***Abstract*— Achieving robust, intuitive, simultaneous and proportional control over multiple degrees of freedom (DOFs) is an outstanding challenge in the development of myoelectric prosthetic systems. Since the priority in myoelectric prosthesis solutions is robustness and stability, their number of functions is usually limited. *Objective:* Here, we introduce a system for intuitive concurrent hand and wrist control, based on a robust feature-extraction protocol and machine-learning. *Methods:* Using the mean absolute value of high-density EMG, we train a ridge-regressor (RR) on only the sustained portions of the single-DOF contractions and leverage the regressor's inherent ability to provide simultaneous multi-DOF estimates. In this way, we robustly capture the amplitude information of the inputs while harnessing the power of the RR to extrapolate otherwise noisy and often overfitted estimations of dynamic portions of movements. *Results:* The real-time evaluation of the system on 13 able-bodied participants and an amputee shows that almost all single-DOF tasks could be reached (96% success rate), while at the same time users were able to complete most of the two-DOF (62%) and even some of the very challenging three-DOF tasks (37%). To further investigate the translational potential of the approach, we reduced the original 192-channel setup to a 16-channel configuration and the observed performance did not deteriorate. Notably, the amputee performed similarly well to the other participants, according to all considered metrics. *Conclusion:* This is the first real-time operated myocontrol system that consistently provides intuitive simultaneous and proportional control over 3-DOFs of wrist and hand, relying on only surface EMG signals from the forearm. *Significance:* Focusing on reduced complexity, a real-time test and the inclusion of an amputee in the study demonstrate the translational potential of the control system for future applications in prosthetic control.**

***Index Terms*— bionics, hand, high-density EMG, myocontrol, prosthetics, ridge-regression, surface EMG**

The study was partially funded by the DFG project *Tact_Hand* (CA-1389/1-1), Academy of Finland project *Hi-Fi BiNDIng* (#333149), and the ERC Synergy project *NaturalBionicS* (#810346).

M. Nowak and C. Castellini are with the German Aerospace Center (DLR), Institute of Robotics and Mechatronics, Wessling, Germany (e-mail: {markus.nowak, claudio.castellini}@dlr.de).

A. Sturma is with the Department of Bioengineering, Imperial College London and the Department of Plastic and Reconstructive Surgery, Medical University of Vienna (e-mail: agnes.sturma@meduniwien.ac.at).

I. Vujaklija is with the Department of Electrical Engineering and Automation, Aalto University (e-mail: ivan.vujaklija@aalto.fi).

D. Farina is with the Department of Bioengineering, Imperial College London (e-mail: d.farina@imperial.ac.uk).

I. Introduction

UPPER limb deficiency is a consequence of traumatic incidents, underlying pathological conditions, comorbidity or a genetic predicament. The resulting functional impairment affects almost every aspect of daily living. For most acquired amputations, and some congenital limb disorders, prosthetic fittings are offered as a primary form of functional support. Most commercially available prosthetic hands provide a small number of selected functions, such as grasping and some form of wrist adjustment, which are controlled individually in a proportional fashion [1]. The most advanced systems rely on the use of surface electromyography (EMG) to establish an interface that decodes the user's motor intent [2].

Commercial myoelectric devices detect EMG signals from an antagonistic pair of remnant muscles (e.g. wrist flexors/extensors) and map them into proportional control of the available prosthetic functions (e.g. gripper open/close) [1]. The access to other available prosthetic degrees of freedom (DOFs), such as wrist rotation, is gained by introducing a switching event that can be determined by a cocontraction or a pulsed signal [3]. While highly robust, this state machine control is unnatural and not suited for restoring dexterous functions. For this reason, myoelectric prostheses have a high rate of abandonment by patients [4].

More recent control approaches consist of EMG signal classification across a finite set of classes (prosthetic functions) [5]–[7] and regression over multiple DOFs [8]. While classification methods usually provide a sequential control (one function at a time), regression-based controllers inherently support concurrent activations of multiple functions. On the other hand, robust regression control of more than two DOFs in transradial amputees has been proven challenging. In Hahne et. al. [9] such a system is investigated in ADL-like assessment tasks. They claim, increasing the number of DOFs to control beyond two becomes unfeasibly due to

increased number of combinations to train [10]. In Ortiz-Catalan et. al. [11] a three-DOF control is reported using a different control approach than the one to be introduced in this work and the one presented by Hahne et. al. [9]. Instead of controlling the position of a prosthesis directly (position control), the velocity to reach a certain DOF configuration is commanded. This allows a wearer to perform a multi-DOF activation either by sequential or simultaneous activation of the involved DOFs. Ortiz-Catalan et. al. [11] do not indicate the amount of simultaneous activation present in reaching two- or three-DOF tasks. In Smith et. al. [12] on the other hand, a further study involving a three-DOF controller, the usage of simultaneity is explicitly investigated. The highest task-specific percentage reported is less than 50% (two-DOF tasks). All these approaches require explicit training of combined activations and only in Hahne et. al. [9] simultaneous two-DOF activation is required to achieve the respective goals.

A further challenge in current myoelectric controllers is the lack of robustness in the presence of instabilities due to altered motor control [13] and methodological factors [14], [15]. Certain academic efforts have been dedicated into tackling this issue [16]–[18] however, a clinically viable solution is yet to be found. At the same time, the induced controller instabilities lead to a lack of predictability which is paramount for establishing an engaging human-machine interface [19]–[21].

Moreover, the usage of more complex control algorithms, e.g. non-linear ones, has not led to significant improvement compared to simpler ones, e.g. linear models [22], [23]. An example of advanced algorithms was presented by Ameri et. al. [24]. The study evaluates a *regression convolutional neural network* offline and in a two-DOF goal-reaching task. Impressive advantages of this approach are a 100% success rate and no need to engineer EMG features. However, these results require training of simultaneous activations (difficult for higher number of DOFs), a velocity control (yet a very high level of simultaneous activation can be seen in the results), and additional engineering required for the design and tuning of the neural network. Furthermore, the possibility for a user to consistently anticipate the behaviour of the controller allows the simpler solutions to harness the power of human motor learning and thus effectively increase the robustness of the interface [25], [26].

Taking all these points into consideration and in order to avoid negative effects of overfitting [27], we propose a three DOFs simultaneous and proportional estimator of wrist and hand actions based on ridge-regression which is trained only on the sustained portions (steady state) of single-DOF contractions, but is tested on multiple activation levels and multi-DOF activation (up to three-DOF combinations). Since our approach resembles a position control scheme, two- and three-DOF targets can *only* be reached using simultaneous activation. Controlling multiple DOFs simultaneously and proportionally has been investigated using high-density EMG under various arrangements employing a velocity control approach, which not necessarily requires simultaneous activation [28], [29].

In this study we focus on the translational potential of our approach. Therefore, we tested the robustness of the performance not only using a high-density EMG with 192 sensors, but also with a reduced sensor arrangement with 16 sensors. Robustness here refers to control stability, e.g. due to changes in the signal during the experiment. The influence of electrode shift or other perturbations are not explicitly tested. To evaluate our approach, we conducted a set of real-time on-screen tests with a group of able-bodied participants and an amputee.

A preliminary version of this work has been reported previously [30].

II. Motion Estimation and Control Algorithm

In order to provide the users with predictable, intuitive and robust myocontrol, the established interface should ideally be consistent and transparent in the way it maps the inputs (the EMG signals) into output control commands (prosthetic motions). This may be achieved by providing as close to linear mapping as possible, and by ensuring system robustness through appropriate signal conditioning and output estimation algorithm design (training) procedure. In this section we describe our proposal for designing this system. We initially describe the EMG signal conditioning, which is followed by the details of the applied motion estimation regression algorithm and the workings of the resulting controller.

EMG signal processing: In order to provide robust inputs to the motion estimation algorithm, the raw acquired EMG signal is filtered by a $5th$ order Butterworth bandpass filter in the frequency range $20Hz-500Hz$. Furthermore, in order to compensate for power-line interference, a $2nd$ order Butterworth band stop filter with cut-off frequencies $45Hz$ and $55Hz$ was applied to the signal. Then, the envelope of the filtered EMG signals was used as input to the regressor. EMG amplitude envelope was selected as it is a robust, commonly used signal feature in myocontrol, which is linearly related to force [31]. The envelope was extracted from the raw EMG by estimates of the root mean square (RMS) values in $100ms$ intervals with an overlap of $90ms$. No channel-wise normalisation was performed, in order to avoid amplification of channels with low signal-to-noise ratio, which could negatively influence the regressor.

Machine Learning: In order to decode user intention, a *Ridge Regression* motion estimation algorithm was employed. The algorithm needs to be trained using representatively labelled EMG data. Contrary to previous regression studies in myocontrol [12], [22], [32], we propose to train the algorithm exclusively on data recorded during steady (constant force) contractions while omitting the dynamic segments from the training set. This approach to training is commonly used with classification methods [33]–[35], but can support users who have difficulties with phantom movements [36], [37]. Here it is chosen in order to reduce the training data variability which reinforces the linear behaviour of the controller, thus potentially increasing the robustness by ensuring the predictability of the controller. Similar ideas have been used to deal with uncertainties in classification approaches [38].

Under the assumption of linearity, the Ridge Regression estimator interpolates the intermediate activations to provide

proportional control and is applied in the following form:

$$\hat{\boldsymbol{y}} = \boldsymbol{W}\boldsymbol{x} \quad \text{with} \quad \boldsymbol{W} = (\boldsymbol{X}^T\boldsymbol{X} + \lambda\boldsymbol{I})^{-1}\boldsymbol{X}^T\boldsymbol{Y} \tag{1}$$

where $\hat{\boldsymbol{y}}$ denotes the predicted hand/wrist DOFs, $\boldsymbol{W}$ are the regression weights, and $\boldsymbol{x}$ denotes a sample of EMG features. Ridge Regression is a regularised version of least-squares regression. The second part in Equation 1 represents the regularisation $\lambda\boldsymbol{I}$, with λ denoting the regularisation parameter and $\boldsymbol{I}$ the identity matrix. The parameter λ was set to 1 as previous studies have indicated this value to be well fit for a wide range of users [37], [39]. The regularisation counters poorly conditioned problems and provides solutions with a lower norm. Furthermore, $\boldsymbol{X}$ stands for the design matrix with all samples of EMG features collected during the algorithm training and $\boldsymbol{Y}$ represents the corresponding hand/wrist configurations. This machine learning (ML) method is one of the fundamental regression techniques, and due to its low computational cost and predictive behaviour it has been used for myoelectric control in previous studies [22], [40]–[42].

Resulting Controller: For the purpose of providing control over multiple DOFs, each DOF is assigned to one regressor, which is trained on both extends of the DOF, e.g. the DOF *wrist rotation* is trained with both *wrist pronation* ($y = 1$) and *wrist supination* ($y = -1$). The output of the controller are real numbers in the range of -1 to 1 and correspond to the activation of a certain DOF rather than to specific forces or joint angles. Therefore, the user is able to utilise the full spectrum of *intermediate* and/or *combined* gesture activations, even though only the *full* activations of *individual* gestures have been collected during ML training. In order to further improve user experience, depending on the personal preferences, either a fifth or a seventh-order moving-average filter was applied to the predicted output values effectively reducing the control jitter. With the windowing of $100ms$ and the delay introduced by the output filtering, the perceived delay remained well under the real-time threshold of $300ms$ [43]. Considering the treatment of the input signals, the applied motion estimation algorithm, and the conditioning of the estimated outputs, the overall control strategy proposed here provides a near-linear translation of EMG readings from the forearm to estimated activations of DOFs of the wrist and hand. A visualisation of the intermediate steps of the resulting controller can be found in the Supplementary Material.

III. Experiment Design and Evaluation

The proposed control algorithm was tested in a real-time virtual environment. The experimental setup included two arrangements with different numbers of EMG channels. The recruited study participants were asked to complete a number of goal-reaching tasks requiring proportional articulation of up to three wrist and hand DOFs concurrently. An extensive analysis of the online performance metrics has been done in order to determine the translational potential of this control approach.

A. Experimental Setup

The main setup components consisted of a high-density EMG acquisition device, a laptop used for computation and execution of the control algorithm, and an external screen used to show visual cues and the online predicted gestures to the participants (Figure 1a).

We recruited 13 able-bodied participants (age 27.5 ± 3, 5 female, 8 male) and one amputee (age 35, male) for the experiments. All participants were provided with a description of the experiment with associated risks and signed an informed consent form after all their questions were answered. The study was approved by the local ethics committee of Imperial College London (ethical approval number: 18IC4685).

Three 8-by-8 ELSCH064NM3 electrode grids were applied around the full circumference of the proximal part of the forearm of each participant. In case of the amputee only two matrices were fitted due to the small dimensions of the residual limb. The acquisition of these 192 monopolar channels (128 for the amputee was realised through a custom made Matlab (Mathworks, Natick, MA, USA) software using the *EMG-USB2+* amplifier by OTBioelettronica (Turin, Italy). Reference electrodes were placed on the wrist of the participants (black band in Figure 1a) and the data acquisition was performed at $2048Hz$.

All computations were performed on a Windows 10 laptop with a $2.2Ghz$ Intel Core i7 CPU and $16GB$ RAM.

B. Experimental Protocol

Based on user surveys [44], six gestures along three DOFs of hand and wrist were selected. These were: *relaxed state*, *power grasp*, *wrist flexion*, *wrist extension*, *wrist pronation* and *wrist supination*.

In order to train the Ridge Regression estimation algorithm, the subjects were first instructed, using the visual cues shown in Figure 1c, to perform three repetitions of the desired gestures at a strong, but comfortable levels of force. During these contractions, only $2s$ of sustained EMG data were recorded and the remaining dynamic portions were excluded. These recordings were then synthetically labelled denoting the cued gesture (no kinematics or kinetics were acquired). No activation (relaxed state) was labelled with $y = 0.0$, while the $2s$ steady-state data was labelled with either $y = 1.0$ (e.g. wrist flexion) or $y = -1.0$ (e.g. wrist extension) depending on the direction of the specific DOF. Any data corresponding to the transition between relaxed and steady state was neglected as previously described.

Upon successful system training, the users were prompted to get familiar with the control and the user interface (UI). After about ten minutes of familiarisation, the participants were instructed to reach different targets on the screen across the DOFs of interest.

These targets were presented to the user in an abstract fashion, as already done in previous studies [45], [46]. This experimental protocol meets the requirements of the later defined Target Achievement Control (TAC) test [47]. Figure 1c shows the goal-reaching UI with two vertical arrows. These arrows were shown on the screen and the user was asked to

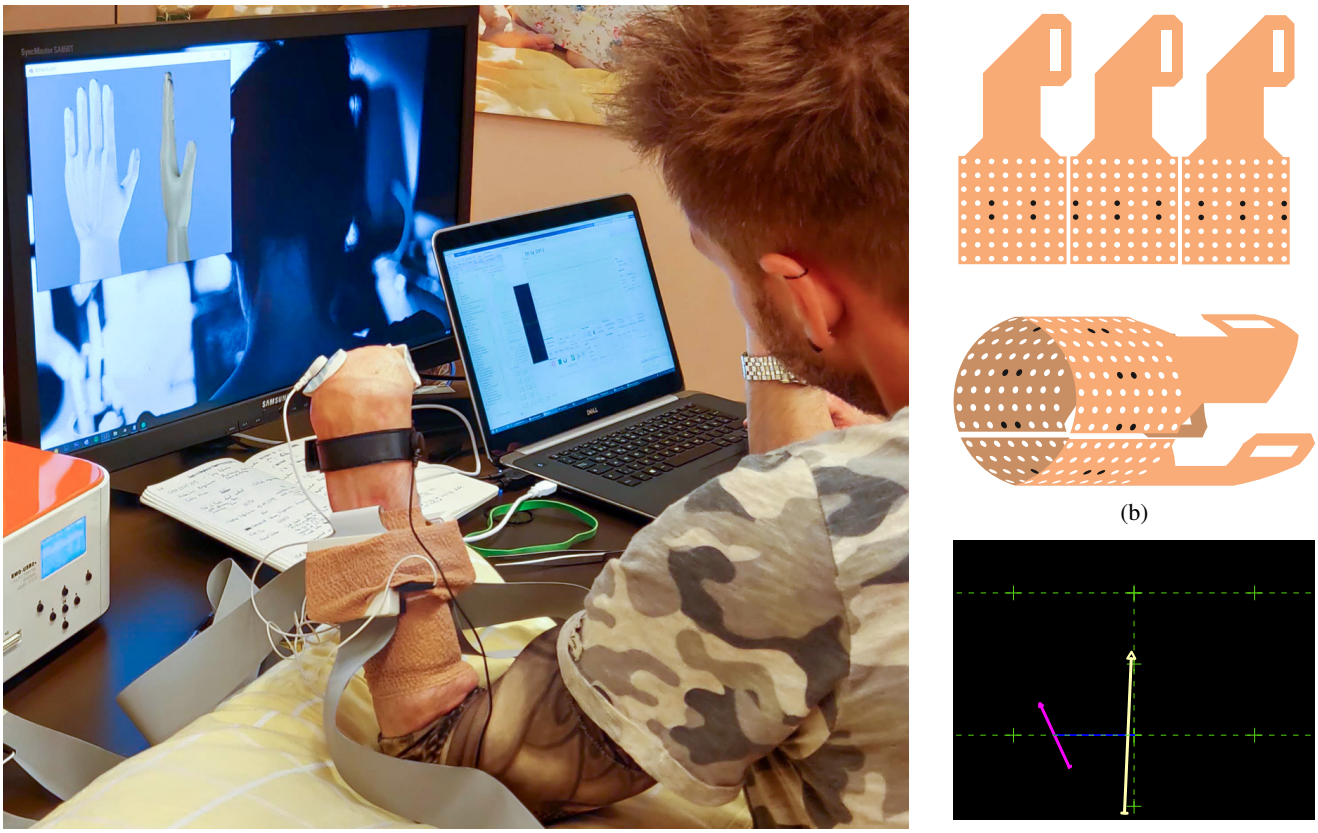

(a) (b) (c)

Fig. 1: Overview of the experimental setup: (a) hardware setup with *EMG-USB2+* amplifier, external screen showing motion prediction and target cue, and participant equipped with two (only in case of amputee, otherwise three) 8x8 sensor matrices; (b) visualisation of the arrangement of the sensor matrices and of the reduced sensor set (highlighted in black); (c) goal-reaching UI: with three-DOF combined target in pink and current prediction in yellow

align them. For each of the DOFs, the arrow would change one of its properties. Translation movement left and right was controlled using the *wrist flexion* and *wrist extension*, rotation was controlled using *wrist pronation* and *wrist supination* and performing a *power grasp* made the arrow shrink. The objective of each task was to reach the target and to remain in its proximity (the error threshold was set to 15% of the normalised work space) for at least $0.3s$. Leaving the target area led to a reset of this dwell time. The user had $20s$ to complete each task, after which the next target was displayed. Reaching the target area was visually indicated to the participant by a change of colour of the arrow from yellow to green. The colour changed back to yellow if the user left the target area. In case the task was not successfully accomplished and the timeout of $20s$ was reached, the colour of the target changed to red and the user was instructed to fully relax before resetting for the next task.

In addition to the arrow representation of the tasks and the control, participants were also shown two hand models. These two hand models, a grey one for the target posture and a beige one for the current prediction, are shown in Figure 1a. However, the users mostly preferred the arrow-based UI.

A total of 24 targets comprised of either individual gestures, such as *power grasp*, or combinations, such as concurrent activation of *power grasp* and *wrist pronation*, were shown to the participants. An added difficulty to the testing was included by introducing intermediate levels of these actions. This was done for both individual gestures, e.g. 30% *wrist pronation*, as well as for combinations, e.g. 30% *wrist pronation* combined with 80% *power grasp*. The targets with the highest difficulty were those which involved a combination of gestures along all three DOFs. Given that the system evaluation focused on the viability of the solution, the overall selection of tasks was based on the ability to conduct robust systematic testing while ensuring not to overburden and fatigue the participants. This meant selecting task activation levels in relation to the increasing difficulty of the concurrent DOF manipulation [47] and thus focusing on the combination levels which are more commonly used during ADLs [48]. A list of gestures used for both training the algorithm and real-time testing is reported in Table I and a visualisation of the execution of ten randomly selected tasks can be found in the Supplementary Material. Furthermore, the Supplementary Material also contains a short clip of the amputee performing a task.

To further test the limits of the approach, four out of the 13 able-bodied participants were selected at random and were asked to perform an additional experiment with a reduced number of sensors and the same 24 goals from Table I. A

TABLE I: Training actions and goals with further categorical information.

		Wr. Fl./Ex.	Wr. Sp./Pr.	Grasp	TargetDoFs	wFlex/Ext	wRot	wGrasp	AccLvl
training data		1.00	0.00	0.00	-	-	-	-	-
		-1.00	0.00	0.00	-	-	-	-	-
		0.00	1.00	0.00	-	-	-	-	-
		0.00	-1.00	0.00	-	-	-	-	-
		0.00	0.00	1.00	-	-	-	-	-
		0.00	0.00	0.00	-	-	-	-	-
testing data	1	0.30	0.00	0.00	1	yes	no	no	0.30
	2	-0.30	0.00	0.00	1	yes	no	no	0.30
	3	0.00	0.30	0.00	1	no	yes	no	0.30
	4	0.00	-0.30	0.00	1	no	yes	no	0.30
	5	0.00	0.00	0.30	1	no	no	yes	0.30
	6	0.00	0.00	0.55	1	no	no	yes	0.55
	7	0.80	0.00	0.00	1	yes	no	no	0.80
	8	-0.80	0.00	0.00	1	yes	no	no	0.80
	9	0.00	0.80	0.00	1	no	yes	no	0.80
	10	0.00	-0.80	0.00	1	no	yes	no	0.80
	11	0.00	0.00	0.80	1	no	no	yes	0.80
	12	0.00	0.00	1.00	1	no	no	yes	1.00
	13	0.55	0.55	0.00	2	yes	yes	no	1.10
	14	0.55	-0.55	0.00	2	yes	yes	no	1.10
	15	-0.55	0.55	0.00	2	yes	yes	no	1.10
	16	-0.55	-0.55	0.00	2	yes	yes	no	1.10
	17	0.55	0.00	0.80	2	yes	no	yes	1.35
	18	-0.55	0.00	0.80	2	yes	no	yes	1.35
	19	0.00	0.55	0.80	2	no	yes	yes	1.35
	20	0.00	-0.55	0.80	2	no	yes	yes	1.35
	21	0.55	0.55	0.80	3	yes	yes	yes	1.90
	22	0.55	-0.55	0.80	3	yes	yes	yes	1.90
	23	-0.55	0.55	0.80	3	yes	yes	yes	1.90
	24	-0.55	-0.55	0.80	3	yes	yes	yes	1.90

reduced set of 16 electrodes was uniformly distributed around the circumference of the forearm in pairs of two channels along the muscle fibres (black dots in Figure 1b).

C. Performance Measures

The primary performance measure was *Success*, which determines whether the participant is able to successfully complete the task of reaching a goal. Successful tasks were further analysed with three secondary performance measures: *TimeToReach*, *Speed* and *PathEfficiency*. *TimeToReach* indicates the time it takes a user to successfully accomplish a task, *Speed* is the ratio between the length of the path travelled and *TimeToReach*, and *PathEfficiency* is the ratio of the length of the shortest path from start (origin of the UI shown in Figure 1c) to endpoint (target location) and the length of the path actually taken by the user.

D. Statistical Evaluation

The primary and each of the three secondary measures were analysed individually. The tasks were chosen to cover several relevant aspects of simultaneous and proportional control. These properties were the independent factors in the statistical evaluation and their values can be found in Table I in columns 6-10 (*TargetDOFs* to *AccLvl*). *TargetDOFs* is a factor with three levels which denote the number of DOFs involved in a task (1 stands for individual gesture goals, while 2 and 3 stand for combinations of 2 or 3 gestures in a goal). *wFlex/Ext*, *wRot* and *wGrasp* indicate whether the corresponding DOF is present in a given task or not. *AccLvl* is the summation of the levels of activation for each gesture involved in a goal. This parameter tells the extent to which each gesture involved in the task should be activated. A further factor (not listed in Table I) is *SensorNumber*, which indicates whether the experiment was conducted with a full set of 192 sensors or the reduced set of 16 sensors.

The statistical analysis was performed for able-bodied participants and only statistical model comparison was done for the amputee data.

The first step was an investigation of the two major factors for evaluating the translational potential of the system, *TargetDOFs* and *SensorNumber*. These can tell how well more complex targets can be reached and how well they can be reached after the number of sensors has been reduced from 192 to 16.

For statistical model fitting of the able-bodied participants' data, all the factors were considered at first, including the interaction terms. In a stepwise process the models have been reduced by removing the factor (and all associated interaction terms) that contributed the least to the explained variance for as long as the reduction was not significantly affecting the corresponding fits. The last non-significant reduction step became the final statistical model, which was followed by post-hoc tests. The post-hoc was a pair-wise *t-test* with *Bonferroni-Correction*.

Finally, these models were extended by the data from the amputee in order to understand whether there was a significant difference.

Due to the nature of the data statistical *Multilevel Modelling* [49]–[53] has been considered. Namely, we have chosen *Linear Mixed-Effects Models* for normally distributed measures and *Generalized Linear Mixed-Effects Models* for *Success*,

which follows a binomial distribution. These methods can deal with unbalanced samples in different groups.

IV. Results

The overview of observed performance across all measures grouped by *TargetDOFs* and *SensorNumber* is shown in Figure 2. The overall success rate with respect to the number of DOFs included in the task is displayed as a bar plot. At the same time, individual measures for *TimeToReach*, *Speed*, and *PathEfficiency* are shown as dots on top of violin plots indicating the distribution of the data. The horizontal line on each violin plot denotes its respective mean and its value is printed in black. Furthermore, all these values (with their standard errors) and the corresponding performance for the amputee participant can be found in Table II.

The performance of the four randomly selected subjects invited to complete the additional experiment with reduced number of sensors has been reported separately. For easier comparison their results for the full sensor configuration and the reduced one are shown side by side ("4 subjects" in Figure 2a). Although the four participants were selected at random, the subset resulted in a group that had a higher success rate than the pool of all participants.

A. Real-time performance analysis

In order to understand different aspects of the observed real-time performance of the system, previously described statistical models were gradually reduced with respect to all outlined factors. The reduction was done until only the factors that had a significant influence on the data remained. The final models were largely similar, yet still feature certain differences for each performance measure:

$$\begin{aligned} \textit{Success} &\sim \textit{TargetDOFs} \\ \log(\textit{TimeToReach}) &\sim \textit{AccLvl} + \textit{wGrasp} \\ \log(\textit{Speed}) &\sim \textit{AccLvl} \\ \textit{PathEfficiency} &\sim \textit{TargetDOFs} + \textit{wGrasp} \end{aligned}$$

From the initial list of six factor introduced in Subsection III-D at most two remain per model. For the performance measure *Success*, only the factor *TargetDOFs* had a significant influence on the *Success* value. Similarly, only *AccLvl* and *wGrasp* significantly influenced *TimeToReach*, only *AccLvl* significantly influenced *Speed* and only *TargetDOFs* and *wGrasp* significantly influenced *PathEfficiency*. As a remark, the factors *TargetDOFs* and *AccLvl* describe similar properties in the models regarding the difficulty of a task. Thus, they could be correlated. Calculating the *Spearman* and *Kendall* correlation confirms this notion with values of $\rho = 0.93$ and $\tau = 0.87$, respectively. Due to the stepwise factor-reduction process the influence of this property should be minimal as the addition to the explained variance is low and therefore one factor is discarded early.

Figure 3 shows the bar plot indicating the subjects' *Success* over different target types, and the violin plots for the performance with respect to the remaining three metrics. However, this time the factors were determined by the statistical model reduction instead of the default ones. Furthermore, brackets in these plots indicate the identified significant pair-wise interactions. The significant interactions are highlighted with asterisks, where '*' stands for $p \in]0.05, 0.01]$, '**' for $p \in]0.01, 0.001]$ and '***' for $p < 0.001$.

When considering the rate of success in reaching different targets, with respect to number of channels used to drive the system, the process of reducing the statistical model showed that there are no statistical differences (Figure 3a, $\chi^2(3) = 5.5346$, $p = 0.1366$ in the stepwise reduction). Similarly, the number of used sensors also had no statistically significant influence on the three secondary performance measures (*TimeToReach*: $\chi^2(10) = 7.1755$, $p = 0.7088$, *Speed*: $\chi^2(7) = 3.5986$, $p = 0.8247$, and *PathEfficiency*: $\chi^2(10) = 14.52$, $p = 0.1506$).

The only factor that did indeed impact the *Success* was the *TargetDOFs*. Targets that only involve one DOF could be reached with a success rate of 96%. However, the performance significantly decreased when the number of DOFs increased from 1 to 2 ($p < 0.001$), from 1 to 3 ($p < 0.001$) and from 2 to 3 ($p = 0.0017$).

The conducted statistical analysis has shown that subjects took significantly longer (Figure 3c, $p < 0.001$) and had a statistically less efficient reaching paths (Figure 3f, $p < 0.001$), when faced with tasks that included power grasp (*wGrasp*). No significant differences were observed in tasks that featured other DOFs (*wFlex/Ext* and *wRot*).

Analysing the data shown in Figure 3b, participants required a significantly shorter time ($p < 0.001$) to complete single DOF tasks that considered the lowest *AccLvl* (0.3) in comparison to those tasks prompting subjects to exert moderate levels of activation (0.8). This was a general trend as the complexity of tasks increased (both in terms of *AccLvl* and *TargetDOFs*).

Similarly, Figure 3d indicates that participants tended to reach higher velocities when they were prompted to complete tasks with higher *AccLvl* and *TargetDOFs*. At the same time, they took significantly less efficient paths ($p < 0.001$) when faced with tasks that involved more than a single DOF. Furthermore

B. Amputee performance

Figure 4 shows the violin plots based on the reduced statistical models for the able-bodied participants overlaid with the individual measurements of the amputee. The horizontal black line representing the mean of the able-bodied participants has now been supplemented with an additional dashed line, indicating the respective mean of the amputee. All these values (with standard errors) and the respective values for the remaining participants are reported in Table II.

This comparison indicated that the amputee subject was as successful as the other subjects ($\chi^2(3) = 2.8011$, $p = 0.4233$). In fact, the overall behaviour was similar with a reduction of the success rate as *TargetDOFs* increased (Figure 4a).

At the same time, he was completing the given tasks at comparable speeds ($\chi^2(7) = 4.379$, $p = 0.7352$). On the other hand, he required significantly more time ($\chi^2(9) = 32.286$, $p < 0.001$) and it took him almost consistently

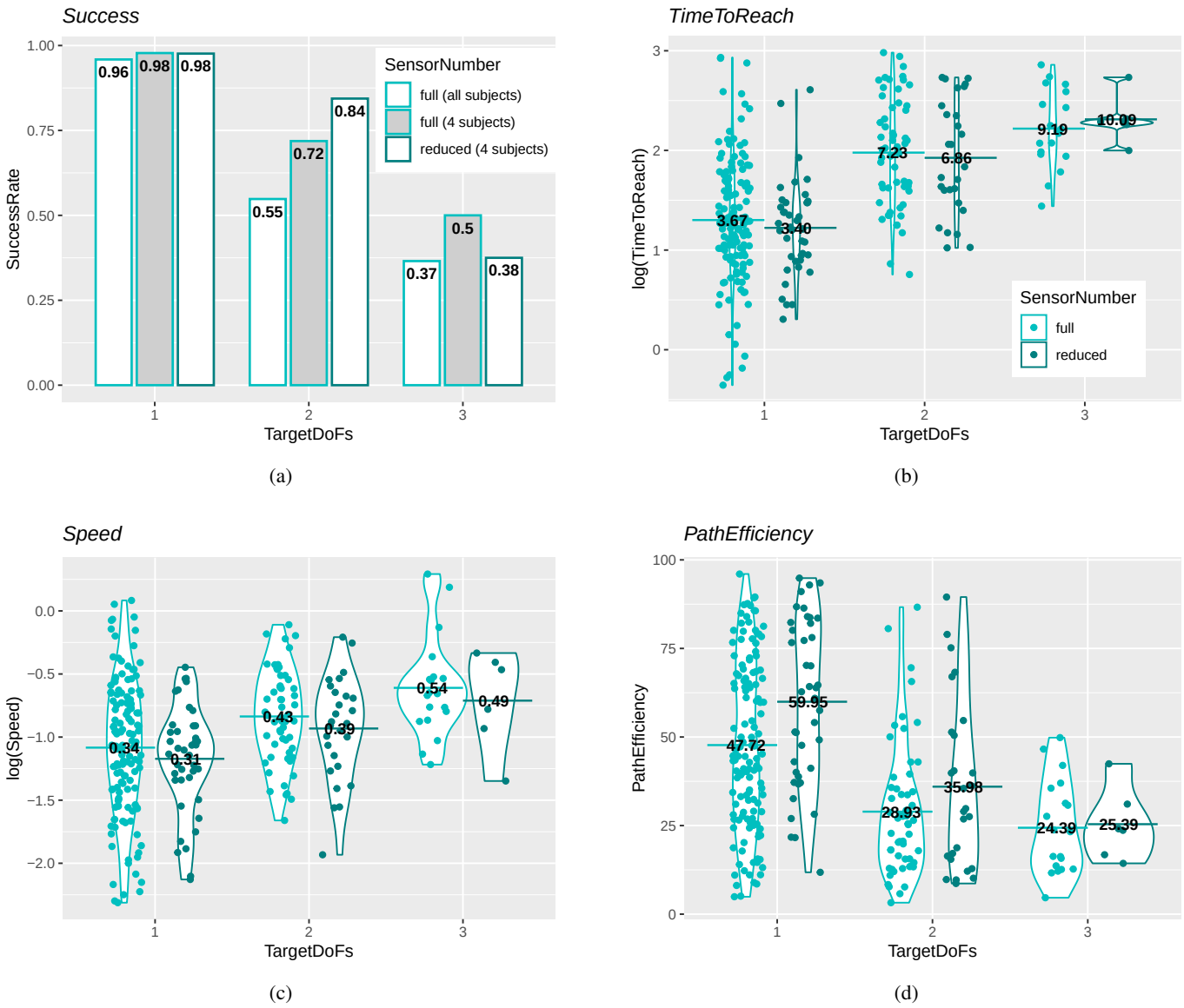

Fig. 2: Overview of the observed performance across four metrics separated by *TargetDOFs* and by *SensorNumber*

longer to complete targets with higher *AccLvl* as seen in Figure 4b. Surprisingly, the amputee subject required less time to complete tasks that included the power grasp (Figure 4c).

Finally, the amputee took significantly longer paths ($\chi^2(4) = 12.031, p = 0.01712$) than other participants, as shown in Figures 4e and 4f.

V. Discussion

In this study we demonstrated real-time simultaneous and proportional myocontrol over three DOFs of hand and wrist using EMG signals from the forearm muscles. The proposed paradigm enables intuitive control by relying on almost linear mapping between input commands and the target output gestures. This is achieved using a simple Ridge Regression motion estimation algorithm trained only on three repetitions of single-DOF steady-state contractions corresponding to the desired motions. The translational potential of this approach has been investigated in real-time experiments with both able-bodied subjects and an amputee, and by eventually reducing the number of EMG channels to a subset of sensors corresponding in number to those present in commercially available prostheses.

Throughout the evaluation of the proposed control algorithm, from the plots shown in Figure 3 and the statistical model analysis presented in Section IV-A, we can conclude that the number of factors that truly influence the control performance is relatively small. Looking into specifics of the observed metrics, there are three main findings to highlight.

First, the proposed approach is capable of extending single DOF control to two and even three DOF control at no additional effort (system training is done only on single-DOF data). The extension to multiple DOF is associated to a decrease in performance in complex tasks, however, the additional capability does not compromise the single-DOF control, which remained at a high success rate. Around

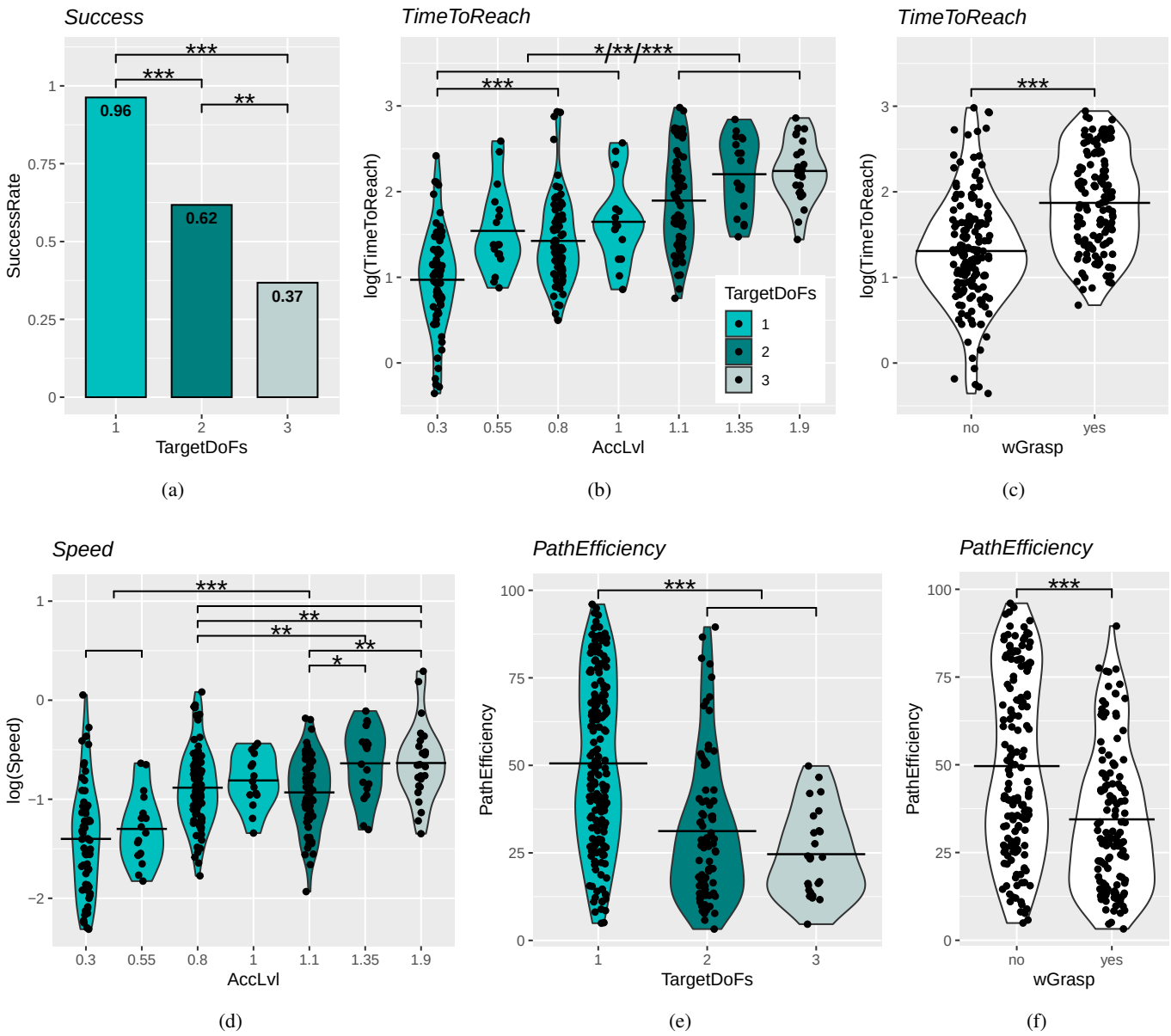

Fig. 3: Final models for all performance measures. Brackets with an asterisk represent significant difference between levels, while brackets without an asterisk represent grouping of different levels. The expression '*/**/***' indicates significant difference between groups with at least $p < 0.05$ for the individual interaction. Significance codes: $p = [0\text{'***'}0.001\text{'**'}0.01\text{'*'}0.05]$

$^2/_3$ of the tasks involving two DOFs and $^1/_3$ of the tasks involving three DOFs could be successfully completed, even though these combinations had not been specifically trained. Furthermore, proportional control over up to three DOFs was achieved without explicitly training on the dynamic portion of the training data. Potential challenges that arise from these training data segments have been linearly interpolated by the controller. Another approach is treating these segments as classes of their own [17], [18]. Similar trends and performance values have been observed previously [54], however, only two DOFs of the wrist have been considered. Barsotti et. al. [40] performed a study only training on individual DOFs and predicting combined activation for up to five finger activations. Both the SR for individual and simultaneous targets are comparable, but lower than in our study, with ca. 85% and ca. 25% respectively for linear feature. Focus of the study has been the comparison between a linear and a non-linear feature. Dealing with combinations of finger activations requires addressing a high level of physiological coupling [39]. Non-linear features can be beneficial in this scenario [40]. These and other more powerful features are potential avenues for improving our control. Furthermore, while a number of studies have used regression for natural combination of DOFs (for an overview see [55]), a simultaneous combination of three DOFs over wrist and hand with proportional capabilities using intuitive mapping has not been experimentally evaluated so far. Smith et. al. [12] and Ortiz-Catalan et. al. [11] have both performed studies regarding simultaneous and proportional control. Both studies have reached success rate similar to ours of more than 90%. These rates have also been achieved

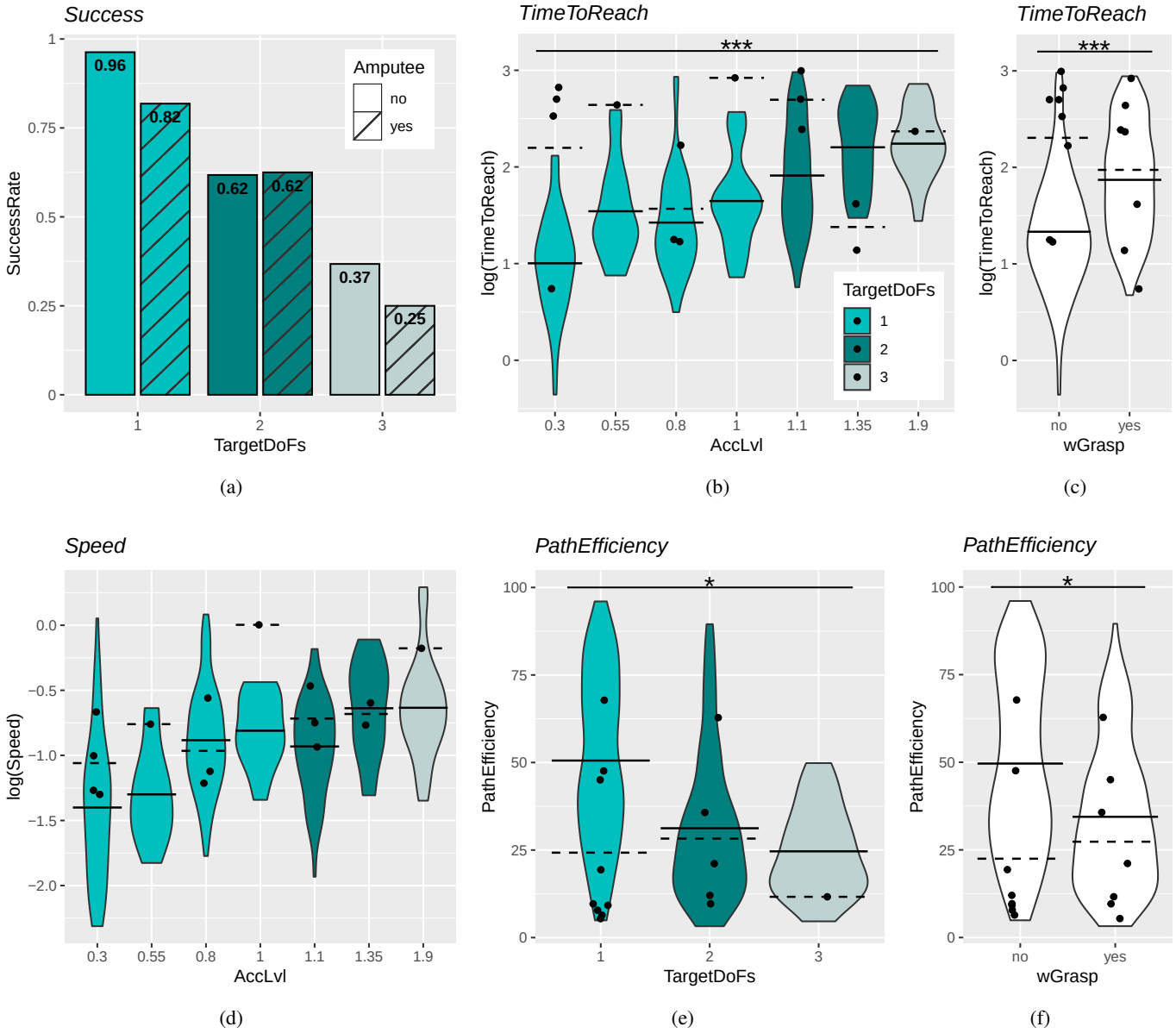

Fig. 4: Final models for the secondary performance measures updated with the performance of the amputee. Full horizontal line represents able-bodied participant sample mean and dashed horizontal line mean of amputee. The violin plots indicating the distribution of the different measure are based on the data of the non-amputee participants. Lines with an asterisk indicate that for this performance measure the difference between the amputee and the remaining participants was significant. Significance codes: $p = [0$ '***' 0.001 '**' 0.01 '*' $0.05]$

in combined tasks, while the performance in our study was significantly lower. However, in said studies the combined activations have been trained explicitly and velocity control was employed. The latter allows the participant to reach multi-DOF targets without using simultaneous activations of these DOFs. Our controller does not require explicit training and yet allows the participants to perform multi-DOF activations. Therefore, in 100% of our multi-DOF tasks simultaneity was used, while simultaneity was used in less than 50% of cases in [12]. Ortiz-Catalan et. al. [11] did not report the usage of simultaneity during target reaching.

Furthermore, it is worth noting that the control over the power grasp (*wGrasp*) seemed to have been more challenging than other gestures for able-bodied subjects and yet easier for the amputee. This was presumably due to a larger variance present in the data related to this movement as it involves more prominent co-activation of different muscle groups. As a further remark, the *power grasp* was the only DOF that had four different levels instead of three for the remaining DOFs. Additional emphasis was put on said DOF due to its importance in prosthetic control. This could have resulted in an unintentional additional difficulty in activating this DOF. On the other hand, the amputee performed better in tasks involving the *power grasp*. An explanation could be that he is a long-term (more than 5 years of daily use) user of a myoelectric prosthesis with hand open and close functionality. Therefore,

TABLE II: Mean values ($\pm$ standard error of the mean, where possible) of the variables indicated in the first column for each combination of *TargetDOFs* and *SensorNumber* for the amputee participant and the remaining participants

Variable	Target DOFs	SensorNumber full	reduced	amputee
SR	1	0.96 ± 0.016	0.98 ± 0.024	0.82 ± 0.12
SR	2	0.55 ± 0.049	0.84 ± 0.065	0.62 ± 0.18
SR	3	0.37 ± 0.067	0.38 ± 0.16	0.25 ± 0.25
log(TTR)	1	1.30 ± 0.052	1.22 ± 0.075	2.12 ± 0.27
log(TTR)	2	1.98 ± 0.072	1.93 ± 0.11	2.17 ± 0.34
log(TTR)	3	2.22 ± 0.089	2.31 ± 0.097	2.37
TTR	1	3.67	3.40	8.31
TTR	2	7.23	6.86	8.75
TTR	3	9.19	10.09	10.68
log(SP)	1	-1.08 ± 0.046	-1.17 ± 0.066	-0.88 ± 0.14
log(SP)	2	-0.84 ± 0.049	-0.93 ± 0.079	-0.70 ± 0.080
log(SP)	3	-0.61 ± 0.091	-0.71 ± 0.16	-0.18
SP	1	0.34	0.31	0.42
SP	2	0.43	0.39	0.50
SP	3	0.54	0.49	0.84
PE	1	47.72 ± 2.02	59.95 ± 3.64	24.25 ± 7.71
PE	2	28.93 ± 2.47	35.98 ± 4.58	28.27 ± 9.77
PE	3	24.39 ± 3.03	25.39 ± 4.18	11.64

while acknowledging that this is a consideration based only on a single subject, the increase in performance on this particular DOF could be attributed to previous training and the frequent, isolated use of the specific muscles related to this particular function.

Second, the performance of the proposed system remained consistent even with a reduced number of input channels. To demonstrate the translational potential of the approach, we decreased the number of EMG channels from 192 to 16 (Figure 1b), which is a number comparable to that of sensors already available in advanced commercial solutions [5], [6]. Although we use the 16 individual sensors in a monopolar configuration, the technical complexity of such a configuration is not significantly different from an 8-channel differential arrangement, as it can be found in said commercial solutions. This reduction in number of electrodes had no significant impact on any of the observed measures. This outcome is consistent with previous work on both regression- and classification-based estimators for myocontrol [46], [56], [57]. Muceli et al. [46] have shown that a channel reduction from 192 to 6 does not negatively influence regression-based user performance, Amma et al. [56] demonstrated that going from 168 to ca. 20 sensors yields a decrease in performance from ca. 95% to ca. 80% and Rojas-Martínez et al. [57] have come to a similar result when reducing from $342-354$ channels to 27. However, our study is the first that successfully demonstrates such resilience during concurrent control of three DOFs of wrist and hand. This is an important observation, since in the process of embedding a myocontroller in a prosthetic device, a lower number of sensors can be beneficial as it drastically reduces the overall technical complexity of the device. An offline analysis further supports the online findings of no significant influence of the sensor reduction. Based on the four subject that participated in the second part of the experiment, we have used the training data of the online experiment to train four regressors with different sensor configurations, i.e. all 192 sensors, the *optimal* 16 sensors, the *optimal* eight sensor pairs, and our uniform configuration of eight sensor pairs. In a repetition-wise three-fold cross-validation we evaluated two measures of fit, i.e. *R2* and *normalised root mean square error (nRMSE)* using a forward search based on *Ridge Regression* adding iteratively the channels that results in the best fit. The results can be found in Table III.

TABLE III: Offline comparison of four sensor configurations, i.e. all 192 sensors, the *optimal* 16 sensors, the *optimal* eight sensor pairs, and uniform configuration of eight sensor pairs, for the four participants of the second part of the experiment assessed using *R2* and *normalised root mean square error (nRMSE)*.

sensor conf.	*R2*	*nRMSE*
192	0.787 ± 0.085	0.195 ± 0.037
opt. 16	0.824 ± 0.084	0.166 ± 0.027
opt. 8 pairs	0.765 ± 0.099	0.191 ± 0.027
uniform 8 pairs	0.597 ± 0.100	0.244 ± 0.018

The uniform sensor configuration has a lower fit of the data then the full sensor configuration or the optimal selection. However, in the online scenario this difference proves not to be significant. Furthermore, the optimal channel selection yields a better fit of the data then the full 192 channels, which could indicate overfit in the full-channel configuration. Since the user-specific optimal channel selection yields a better fit than the uniform selection, a potential improvement could be achieved with individual sensor placement per user.

Third, while using the proposed control approach an amputee was similarly successful in completing the presented tasks as other subjects. However, he took longer to complete them and his *PathEfficiency* was lower than the one from the remaining participants. While these results have to be considered cautiously since based on a single patient, they indicate that the proposed system has the potential to be used by amputees.

Beyond these main findings, from Figures 3d and 3e it could be argued that for higher *AccLvl* the oscillation and the instability of the provided control increases. This could be explained by the fact that with increasing *AccLvl*, and therefore also with a rise in number of DOFs that need to be addressed (*TargetDOFs*), the user has to navigate the controller in an area where the algorithm was not explicitly trained. This potentially leads to a more jittery behaviour, which is emphasized by the fact that there is no significant difference for *PathEfficiency* between two- and three-DOF tasks. System training data only consisted of single-DOF motions, thus when reaching for the targets that require combined movements, the control may become more unstable. Besides the influence of the training data a reduced *PathEfficiency* can also be explained by physiological aspects. A theoretical combination of e.g. *wrist flexion* and *power grasp* at their maximum voluntary contraction (MVC) is physiologically not possible [58]. These properties have been taken into account for the design of the goal-reaching tasks. However, specific combinations can pose added difficulty and could require less efficient reaching paths. Physiological aspects could explain

the different performance for tasks involving the *power grasp*. Potentially, this unstable behaviour could be alleviated by the user gaining more experience with the controller [26] or an incremental learning scheme [41] to update training data when needed. Nevertheless, the benefit of having a very simple and quick system training, and the fact that single-DOF control remains high with combined actions still well handled, arguably outweighs the observed reduction in performance.

VI. Conclusion

We have proposed and demonstrated a system for simultaneous and proportional real-time EMG control over 3-DOFs with an intuitive interface, and minimal user and machine training. This was done by training a Ridge Regression algorithm solely on steady portions of three repetitions of the single DOF dynamic contractions of wrist and hand. Such design choice has allowed us to reduce the influence of data variability introduced by dynamic inputs and to leverage on the simplicity of the estimator.

References

[1] I. Vujaklija, D. Farina, and O. Aszmann, "New developments in prosthetic arm systems," *Orthopedic Research and Reviews*, vol. Volume 8, pp. 31–39, Jul. 2016.

[2] N. Jiang, S. Dosen, K.-R. Muller, and D. Farina, "Myoelectric Control of Artificial Limbs—Is There a Need to Change Focus? [In the Spotlight]," *IEEE Signal Processing Magazine*, vol. 29, no. 5, pp. 152–150, Sep. 2012.

[3] R. N. Scott and P. A. Parker, "Myoelectric Prostheses: State of the art," *Journal of Medical Engineering & Technology*, vol. 12, no. 4, pp. 143–151, Jan. 1988.

[4] E. Biddiss and T. Chau, "Upper-Limb Prosthetics: Critical Factors in Device Abandonment," *American Journal of Physical Medicine & Rehabilitation*, vol. 86, no. 12, pp. 977–987, Dec. 2007.

[5] Coapt LLC, "COMPLETE CONTROL Handbook," 2018.

[6] Ottobock, "Technology for people 4.0: Ottobock at OTWorld 2018," https://www.ottobock.com/en/newsroom/news/technology-for-people-4-0-ottobock-at-otworld-2018.html, May 2018.

[7] E. Scheme and K. Englehart, "Electromyogram pattern recognition for control of powered upper-limb prostheses: State of the art and challenges for clinical use," *The Journal of Rehabilitation Research and Development*, vol. 48, no. 6, p. 643, 2011.

[8] I. Vujaklija, "Novel Control Strategies for Upper Limb Prosthetics," in *Converging Clinical and Engineering Research on Neurorehabilitation III*, ser. Biosystems & Biorobotics, L. Masia, S. Micera, M. Akay, and J. L. Pons, Eds. Cham: Springer International Publishing, 2019, pp. 171–174.

[9] J. M. Hahne, M. A. Schweisfurth, M. Koppe, and D. Farina, "Simultaneous control of multiple functions of bionic hand prostheses: Performance and robustness in end users," *Science Robotics*, vol. 3, no. 19, Jun. 2018.

[10] J. M. Hahne, S. Dahne, H.-J. Hwang, K.-R. Muller, and L. C. Parra, "Concurrent Adaptation of Human and Machine Improves Simultaneous and Proportional Myoelectric Control," *IEEE Transactions on Neural Systems and Rehabilitation Engineering*, vol. 23, no. 4, pp. 618–627, Jul. 2015.

[11] M. Ortiz-Catalan, B. Håkansson, and R. Brånemark, "Real-Time and Simultaneous Control of Artificial Limbs Based on Pattern Recognition Algorithms," *IEEE Transactions on Neural Systems and Rehabilitation Engineering*, vol. 22, no. 4, pp. 756–764, Jul. 2014.

[12] L. H. Smith, T. A. Kuiken, and L. J. Hargrove, "Evaluation of Linear Regression Simultaneous Myoelectric Control Using Intramuscular EMG," *IEEE Transactions on Biomedical Engineering*, vol. 63, no. 4, pp. 737–746, Apr. 2016.

[13] V. Glaser and A. Holobar, "Motor Unit Identification From High-Density Surface Electromyograms in Repeated Dynamic Muscle Contractions," *IEEE Transactions on Neural Systems and Rehabilitation Engineering*, vol. 27, no. 1, pp. 66–75, Jan. 2019.

[14] C. J. De Luca, S.-S. Chang, S. H. Roy, J. C. Kline, and S. H. Nawab, "Decomposition of surface EMG signals from cyclic dynamic contractions," *Journal of Neurophysiology*, vol. 113, no. 6, pp. 1941–1951, Dec. 2014.

[15] L. Hargrove, Y. Losier, B. Lock, K. Englehart, and B. Hudgins, "A Real-Time Pattern Recognition Based Myoelectric Control Usability Study Implemented in a Virtual Environment," in *2007 29th Annual International Conference of the IEEE Engineering in Medicine and Biology Society*, Aug. 2007, pp. 4842–4845.

[16] K. Englehart, B. Hudgins, P. A. Parker, and M. Stevenson, "Classification of the myoelectric signal using time-frequency based representations," *Medical Engineering & Physics*, vol. 21, no. 6, pp. 431–438, Jul. 1999.

[17] G. Kanitz, C. Cipriani, and B. B. Edin, "Classification of Transient Myoelectric Signals for the Control of Multi-Grasp Hand Prostheses," *IEEE Transactions on Neural Systems and Rehabilitation Engineering*, vol. 26, no. 9, pp. 1756–1764, Sep. 2018.

[18] M. Stachaczyk, S. F. Atashzar, S. Dupan, I. Vujaklija, and D. Farina, "Multiclass Detection and Tracking of Transient Motor Activation based on Decomposed Myoelectric Signals," in *2019 9th International IEEE/EMBS Conference on Neural Engineering (NER)*, Mar. 2019, pp. 1080–1083.

[19] D. Farina, I. Vujaklija, R. Brånemark, A. M. J. Bull, H. Dietl, B. Graimann, L. J. Hargrove, K.-P. Hoffmann, H. H. Huang, T. Ingvarsson, H. B. Janusson, K. Kristjánsson, T. Kuiken, S. Micera, T. Stieglitz, A. Sturma, D. Tyler, R. F. ff Weir, and O. C. Aszmann, "Toward higher-performance bionic limbs for wider clinical use," *Nature Biomedical Engineering*, pp. 1–13, May 2021.

[20] C. Castellini, R. M. Bongers, M. Nowak, and C. K. van der Sluis, "Upper-Limb Prosthetic Myocontrol: Two Recommendations," *Frontiers in Neuroscience*, vol. 9, 2016.

[21] D. Yeung, I. Mendez Guerra, I. Barner-Rasmussen, E. Siponen, D. Farina, and I. Vujaklija, "Co-adaptive control of bionic limbs via unsupervised adaptation of muscle synergies," *IEEE Transactions on Biomedical Engineering*, pp. 1–1, 2022.

[22] J. M. Hahne, F. Biebmann, N. Jiang, H. Rehbaum, D. Farina, F. C. Meinecke, K.-R. Muller, and L. C. Parra, "Linear and Nonlinear Regression Techniques for Simultaneous and Proportional Myoelectric Control," *IEEE Transactions on Neural Systems and Rehabilitation Engineering*, vol. 22, no. 2, pp. 269–279, Mar. 2014.

[23] J. M. Hahne, M. Markovic, and D. Farina, "User adaptation in Myoelectric Man-Machine Interfaces," *Scientific Reports*, vol. 7, no. 1, p. 4437, Jun. 2017.

[24] A. Ameri, M. A. Akhaee, E. Scheme, and K. Englehart, "Regression convolutional neural network for improved simultaneous EMG control," *Journal of Neural Engineering*, vol. 16, no. 3, p. 036015, Jun. 2019.

[25] M. Ison and P. Artemiadis, "Proportional Myoelectric Control of Robots: Muscle Synergy Development Drives Performance Enhancement, Retainment, and Generalization," *IEEE Transactions on Robotics*, vol. 31, no. 2, pp. 259–268, Apr. 2015.

[26] A. Krasoulis, S. Vijayakumar, and K. Nazarpour, "Effect of User Practice on Prosthetic Finger Control With an Intuitive Myoelectric Decoder," *Frontiers in Neuroscience*, vol. 13, 2019.

[27] D. M. Hawkins, "The Problem of Overfitting," *Journal of Chemical Information and Computer Sciences*, vol. 44, no. 1, pp. 1–12, Jan. 2004.

[28] M. Ison, I. Vujaklija, B. Whitsell, D. Farina, and P. Artemiadis, "High-Density Electromyography and Motor Skill Learning for Robust Long-Term Control of a 7-DoF Robot Arm," *IEEE Transactions on Neural Systems and Rehabilitation Engineering*, vol. 24, no. 4, pp. 424–433, Apr. 2016.

[29] S. Muceli and D. Farina, "Simultaneous and Proportional Estimation of Hand Kinematics From EMG During Mirrored Movements at Multiple Degrees-of-Freedom," *IEEE Transactions on Neural Systems and Rehabilitation Engineering*, vol. 20, no. 3, pp. 371–378, May 2012.

[30] M. Nowak, I. Vujaklija, C. Castellini, and D. Farina, "Highly Intuitive 3-DOF Simultaneous and Proportional Myocontrol of Wrist and Hand," in *In Press*, Oct. 2020, p. 2.

[31] D. Farina, R. Merletti, and R. M. Enoka, "The extraction of neural strategies from the surface EMG," *Journal of Applied Physiology*, vol. 96, no. 4, pp. 1486–1495, Apr. 2004.

[32] L. H. Smith, T. A. Kuiken, and L. J. Hargrove, "Linear regression using intramuscular EMG for simultaneous myoelectric control of a wrist and hand system," in *2015 7th International IEEE/EMBS Conference on Neural Engineering (NER)*, Apr. 2015, pp. 619–622.

[33] K. Englehart and B. Hudgins, "A robust, real-time control scheme for multifunction myoelectric control," *IEEE Transactions on Biomedical Engineering*, vol. 50, no. 7, pp. 848–854, Jul. 2003.

[34] T. A. Kuiken, G. Li, B. A. Lock, R. D. Lipschutz, L. A. Miller, K. A. Stubblefield, and K. B. Englehart, "Targeted muscle reinnervation for real-time myoelectric control of multifunction artificial arms," *Jama*, vol. 301, no. 6, pp. 619–628, 2009.

[35] A. J. Young, L. H. Smith, E. J. Rouse, and L. J. Hargrove, "Classification of Simultaneous Movements Using Surface EMG Pattern Recognition," *IEEE Transactions on Biomedical Engineering*, vol. 60, no. 5, pp. 1250–1258, May 2013.

[36] D. Sierra González and C. Castellini, "A realistic implementation of ultrasound imaging as a human-machine interface for upper-limb amputees," *Frontiers in Neurorobotics*, vol. 7, 2013.

[37] A. Gijsberts, R. Bohra, D. Sierra González, A. Werner, M. Nowak, B. Caputo, M. A. Roa, and C. P. D. Castellini, "Stable myoelectric control of a hand prosthesis using non-linear incremental learning," *Frontiers in Neurorobotics*, vol. 8, 2014.

[38] G. K. Patel, C. Castellini, J. M. Hahne, D. Farina, and S. Dosen, "A Classification Method for Myoelectric Control of Hand Prostheses Inspired by Muscle Coordination," *IEEE Transactions on Neural Systems and Rehabilitation Engineering*, vol. 26, no. 9, pp. 1745–1755, Sep. 2018.

[39] M. Nowak and C. Castellini, "The LET Procedure for Prosthetic Myocontrol: Towards Multi-DOF Control Using Single-DOF Activations," *PLOS ONE*, vol. 11, no. 9, p. e0161678, Sep. 2016.

[40] M. Barsotti, S. Dupan, I. Vujaklija, S. Došen, A. Frisoli, and D. Farina, "Online Finger Control Using High-Density EMG and Minimal Training Data for Robotic Applications," *IEEE Robotics and Automation Letters*, vol. 4, no. 2, pp. 217–223, Apr. 2019.

[41] I. Strazzulla, M. Nowak, M. Controzzi, C. Cipriani, and C. Castellini, "Online Bimanual Manipulation Using Surface Electromyography and Incremental Learning," *IEEE Transactions on Neural Systems and Rehabilitation Engineering*, vol. 25, no. 3, pp. 227–234, Mar. 2017.

[42] M. Nowak, T. Eiband, E. Ruiz Ramírez, and C. Castellini, "Action interference in simultaneous and proportional myocontrol: Comparing force- and electromyography," *Journal of Neural Engineering*, vol. 17, no. 2, p. 026011, Mar. 2020.

[43] T. R. Farrell and R. F. Weir, "The Optimal Controller Delay for Myoelectric Prostheses," *IEEE Transactions on Neural Systems and Rehabilitation Engineering*, vol. 15, no. 1, pp. 111–118, Mar. 2007.

[44] F. Cordella, A. L. Ciancio, R. Sacchetti, A. Davalli, A. G. Cutti, E. Guglielmelli, and L. Zollo, "Literature Review on Needs of Upper Limb Prosthesis Users," *Frontiers in Neuroscience*, vol. 10, 2016.

[45] H. Rehbaum, N. Jiang, L. Paredes, S. Amsuess, B. Graimann, and D. Farina, "Real time simultaneous and proportional control of multiple degrees of freedom from surface EMG: Preliminary results on subjects with limb deficiency," in *2012 Annual International Conference of the IEEE Engineering in Medicine and Biology Society*, Aug. 2012, pp. 1346–1349.

[46] S. Muceli, N. Jiang, and D. Farina, "Extracting Signals Robust to Electrode Number and Shift for Online Simultaneous and Proportional Myoelectric Control by Factorization Algorithms," *IEEE Transactions on Neural Systems and Rehabilitation Engineering*, vol. 22, no. 3, pp. 623–633, May 2014.

[47] A. M. Simon, L. J. Hargrove, B. A. Lock, and T. A. Kuiken, "The Target Achievement Control Test: Evaluating real-time myoelectric pattern-recognition control of multifunctional upper-limb prostheses," *The Journal of Rehabilitation Research and Development*, vol. 48, no. 6, p. 619, 2011.

[48] J. Ryu, W. P. Cooney, L. J. Askew, K.-N. An, and E. Y. Chao, "Functional ranges of motion of the wrist joint," *The Journal of Hand Surgery*, vol. 16, no. 3, pp. 409–419, May 1991.

[49] A. P. Field, J. Miles, and Z. Field, *Discovering Statistics Using R*. London ; Thousand Oaks, Calif: Sage, 2012.

[50] W. H. Finch, J. E. Bolin, and K. Kelley, *Multilevel Modeling Using R*. New York: Crc Press, 2019.

[51] T. A. Snijders and R. J. Bosker, *Multilevel Analysis: An Introduction to Basic and Advanced Multilevel Modeling*. Sage, 2011.

[52] D. A. Powers, "Multilevel models for binary data," *New Directions for Institutional Research*, vol. 2012, no. 154, pp. 57–75, 2012.

[53] C. J. Anderson, J.-S. Kim, and B. Keller, "Multilevel Modeling of Categorical Response Variables," 2014, p. 39.

[54] A. Pradhan, N. Jiang, V. Chester, and U. Kuruganti, "Linear regression with frequency division technique for robust simultaneous and proportional myoelectric control during medium and high contraction-level variation," *Biomedical Signal Processing and Control*, vol. 61, p. 101984, Aug. 2020.

[55] C. Igual, L. A. Pardo, J. M. Hahne, and J. Igual, "Myoelectric Control for Upper Limb Prostheses," *Electronics*, vol. 8, no. 11, p. 1244, Nov. 2019.

[56] C. Amma, T. Krings, J. Böer, and T. Schultz, "Advancing Muscle-Computer Interfaces with High-Density Electromyography," in *Proceedings of the 33rd Annual ACM Conference on Human Factors in Computing Systems*, ser. CHI '15. New York, NY, USA: Association for Computing Machinery, Apr. 2015, pp. 929–938.

[57] M. Rojas-Martínez, M. Mañanas, J. Alonso, and R. Merletti, "Identification of isometric contractions based on High Density EMG maps," *Journal of Electromyography and Kinesiology*, vol. 23, no. 1, pp. 33–42, Feb. 2013.

[58] M. Connan, R. Kõiva, and C. Castellini, "Online Natural Myocontrol of Combined Hand and Wrist Actions Using Tactile Myography and the Biomechanics of Grasping," *Frontiers in Neurorobotics*, vol. 14, p. 11, Feb. 2020.